eLIFE
elifesciences.org

RESEARCH ARTICLE

Figures and figure supplements

Dual control of NAD^+ synthesis by purine metabolites in yeast

Benoît Pinson *et al*

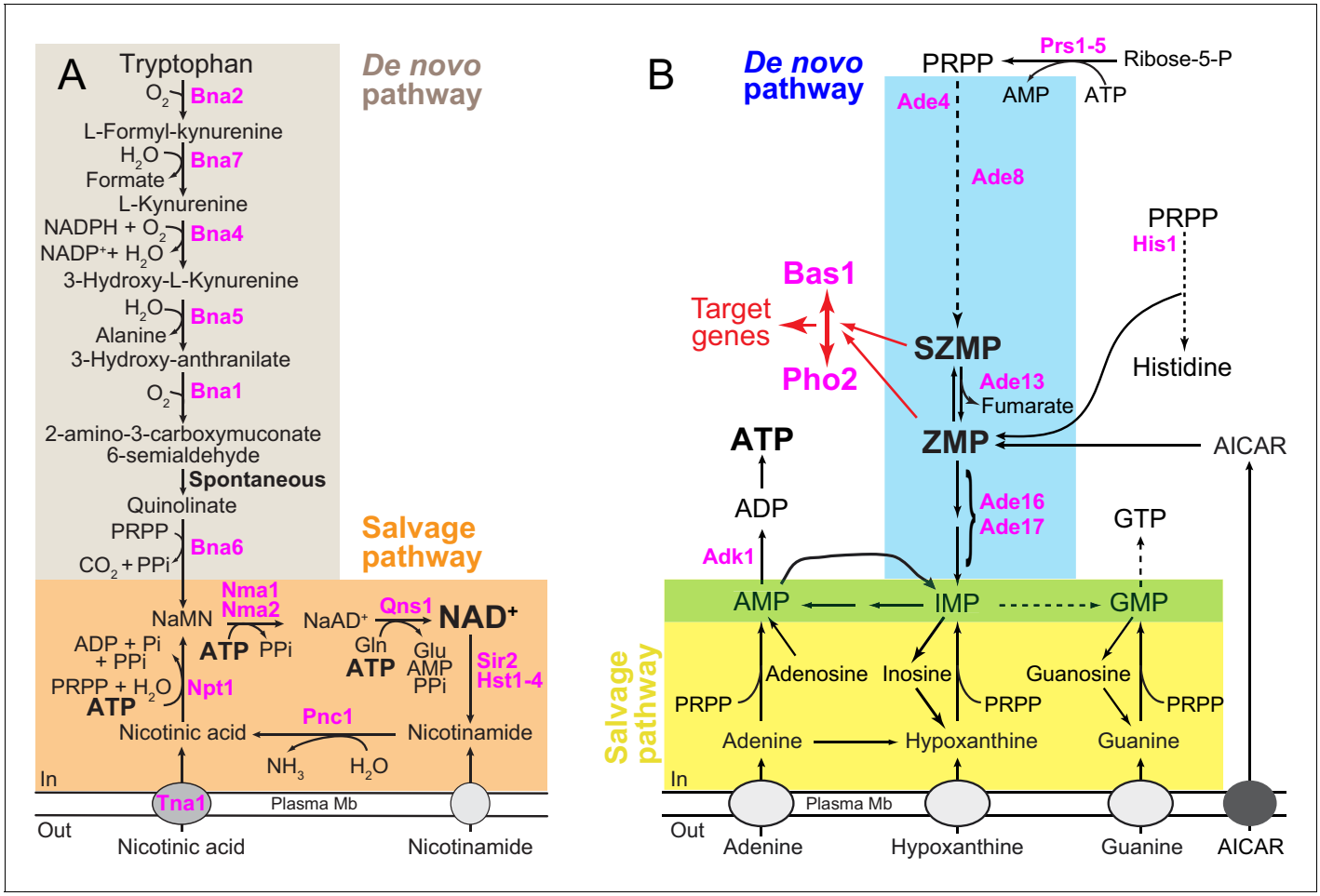

Figure 1. Schematic representation of the yeast pyridine and purine biosynthesis pathways. (**A**) NAD^+ de novo and salvage pathways in yeast. $NaAD^+$: nicotinic acid adenine dinucleotide; NADP: nicotinamide adenine dinucleotide phosphate; NaMN: nicotinic acid mononucleotide; Pi: inorganic phosphate; PPi: pyrophosphate and PRPP: 5-phosphoribosyl-1-pyrophosphate. (**B**) Purine de novo and salvage pathways in yeast. AICAR: 5-amino-4-imidazole carboxamide ribonucleoside; IMP: inosine 5′-mono-phosphate; SZMP: succinyl-ZMP and ZMP: 5-amino-4-imidazole carboxamide ribonucleotide 5′-phosphate. Red arrows illustrate the (S)ZMP-dependent Bas1/Pho2 interaction leading to the transcriptional regulation of their target genes. IMP conversion onto either AMP or GMP is common to the de novo and salvage pathways (green box). (**A–B**) Only the proteins mentioned in the text are shown (in pink).

DOI: https://doi.org/10.7554/eLife.43808.002

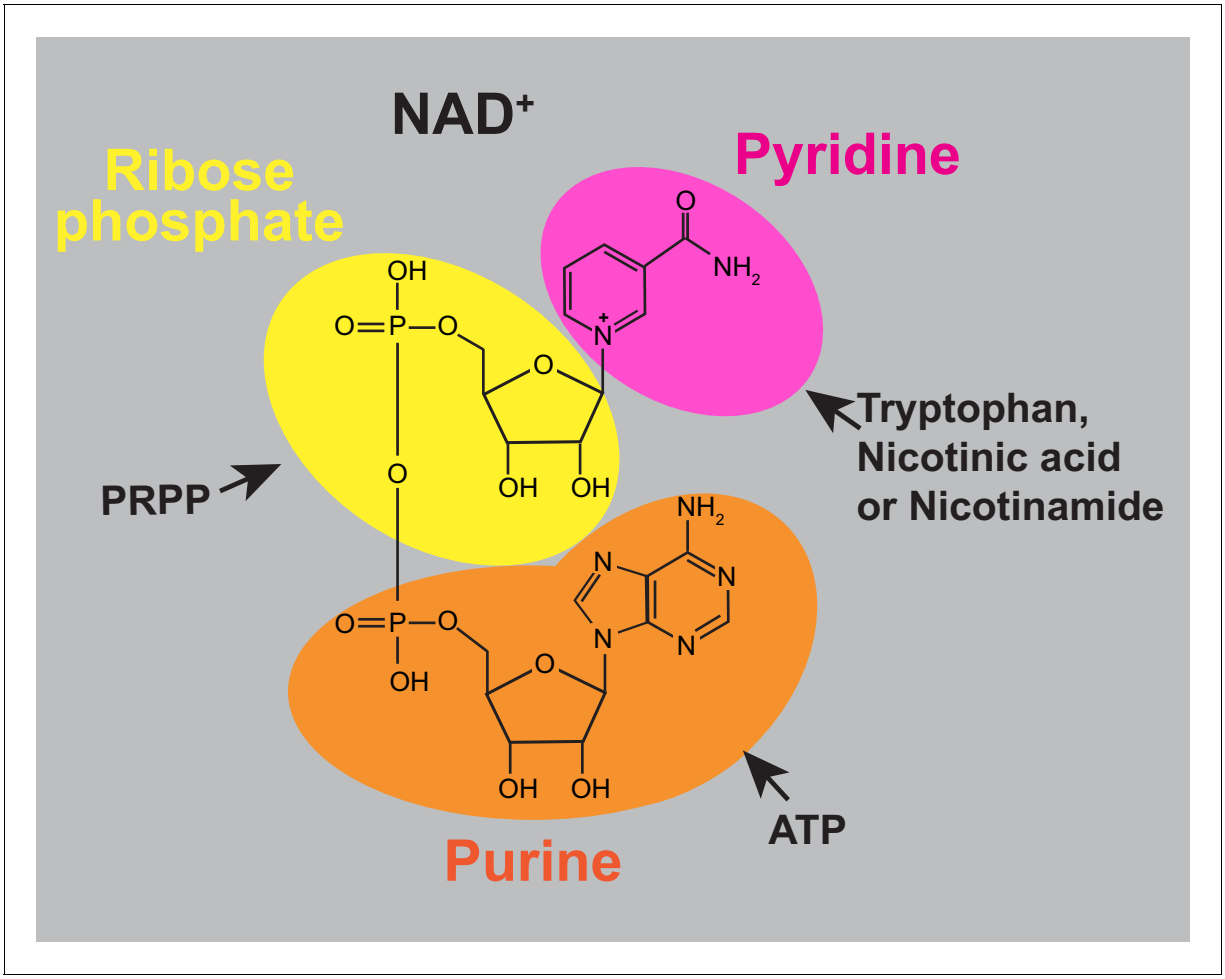

Figure 1—figure supplement 1. Chemical structure of NAD^+. Colored areas highlight the precursor metabolites in the NAD^+ backbone. Pink area: Pyridine ring coming from tryptophan (via the pyridine de novo pathway), nicotinic acid and/or nicotinamide (via the pyridine salvage pathway). Yellow area: Ribose phosphate moiety resulting from 5-phosphoribosyl pyrophosphate (PRPP) incorporation by phosphoribosyl transferases. Orange area: Adenine nucleotide part arising from ATP incorporation at the step catalyzed by the nicotinic acid mononucleotide transferases.

DOI: https://doi.org/10.7554/eLife.43808.003

Figure 2. NAD$^+$precursors and biosynthesis intermediates respond to variations in extracellular purine availability. The prototrophic wild-type strain FY4 was kept in exponential phase for 24 hr in SDcasaWU medium supplemented (red dots) or not (blue dots) with extracellular adenine. Metabolites were then extracted and separated by liquid chromatography. Quantifications were determined on independent metabolite extractions (Biological replicates; N ≥ 5) and standard deviation is presented. For each metabolite, the amount measured in cells grown in the presence of adenine (red dots) was set at 1. Numbers on the top of each panel correspond to the p-value calculated from a Welch's unpaired t-test.

DOI: https://doi.org/10.7554/eLife.43808.004

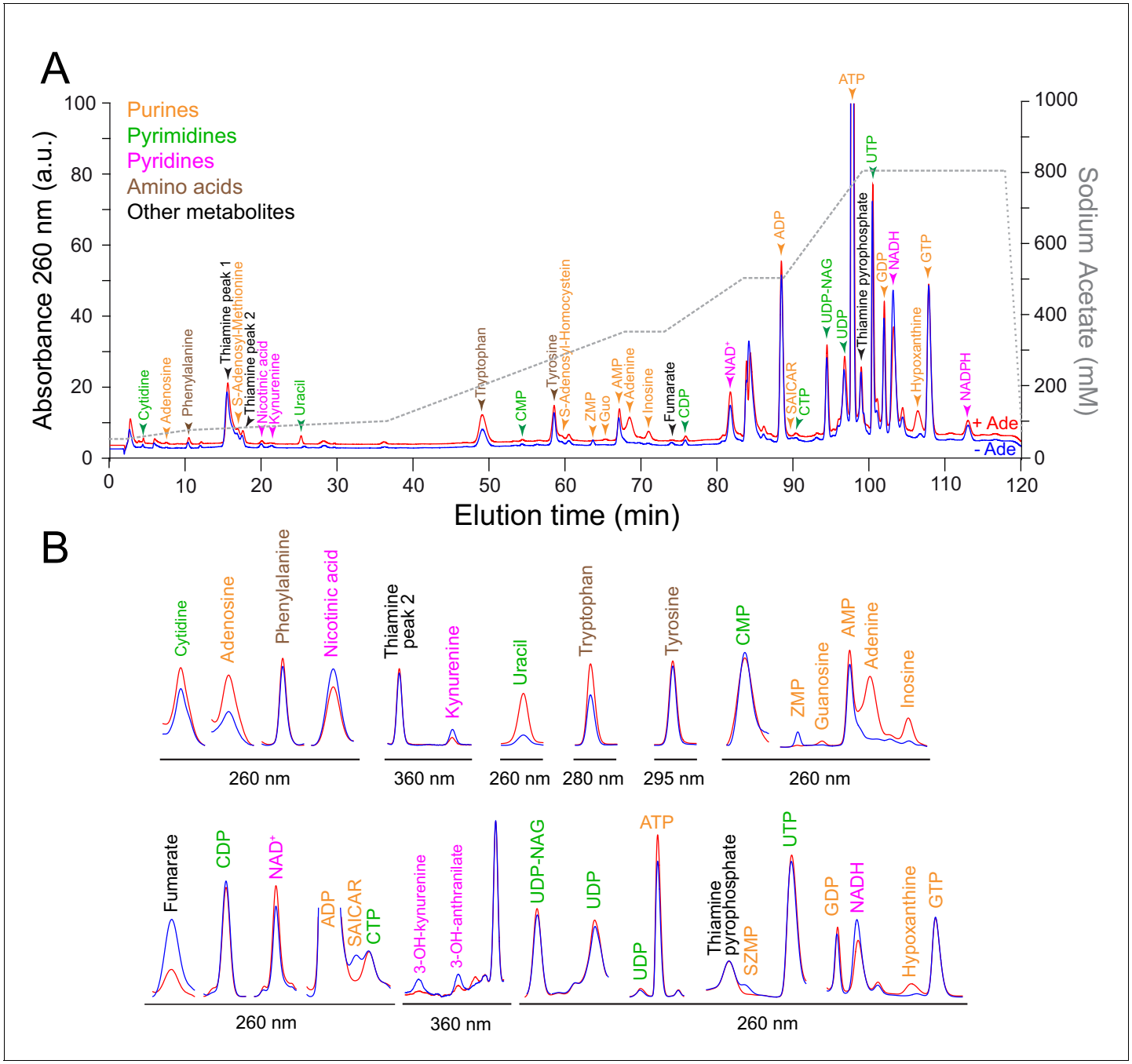

Figure 2—figure supplement 1. Separation of intracellular metabolites by high-performance ion chromatography. A prototrophic yeast strain (FY4) was grown in SDcasaWU medium ±Adenine. Metabolite extraction and separation by liquid chromatography were performed as described in the Materials and methods section. (**A**) Typical entire chromatograms obtained at 260 nm in the presence (red line) or the absence (blue line) of external adenine (Ade). Similar patterns were found in all metabolic extractions presented in ***Figure 2***. Identified peaks are indicated with a color code corresponding to metabolite families. (**B**) Zooms of absorbance signals obtained from chromatogram at indicated wavelengths. ADP: adenosine 5'-diphosphate, AMP: adenosine 5'-monophosphate, ATP: adenosine 5'-triphosphate, CDP: cytidine 5'-diphosphate, CMP: cytidine 5'-monophosphate, CTP: cytidine 5'-triphosphate, GDP: guanosine 5'-diphosphate, GTP: guanosine 5'-triphosphate, NAD^+: nicotinamide adenine dinucleotide, NADH: nicotinamide adenine dinucleotide reduced form, NADPH: phosphorylated form of NADH, SAICAR: succinyl-aminoimidazole carboxamide ribonucleoside, UDP: uridine 5'-diphosphate, UDP-NAG: uridine 5'-diphosphate-N-acetyl glucosamine, UTP: uridine 5'-triphosphate, ZMP: 5-amino-4-imidazole carboxamide ribonucleotide 5'-phosphate and SZMP: succinyl-ZMP.

DOI: https://doi.org/10.7554/eLife.43808.005

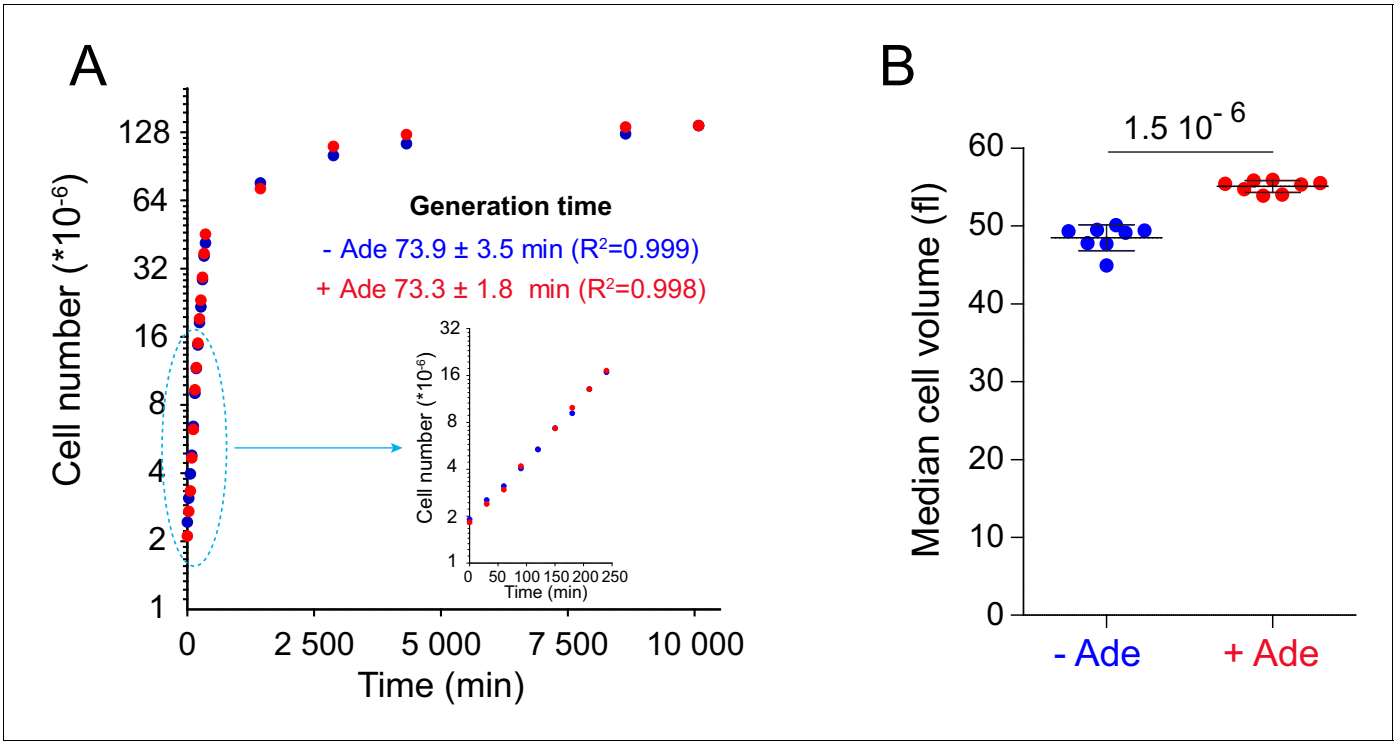

Figure 2—figure supplement 2. Adenine supplementation affects cell growth but not cell proliferation. (**A**) A prototrophic yeast strain (FY4) was exponentially grown for 24 hr in SDcasaWU medium ±Adenine as in ***Figure 2***. Cultures were then diluted at 2 10^6 cells/ml and cell number was followed by using a Multisizer IV (Beckman Coulter). Generation time was determined with a non-linear growth fit (GraphPad Prism) on cells grown in the presence (red dots) or the absence (blue dots) of adenine (N = 2). (**B**) Median cell volume was determined on the independent exponentially grown cells (N = 8) used for the metabolic extraction presented in ***Figure 8A–D***. Number on the top corresponds to the p-value calculated from a Welch's t-test.

DOI: https://doi.org/10.7554/eLife.43808.006

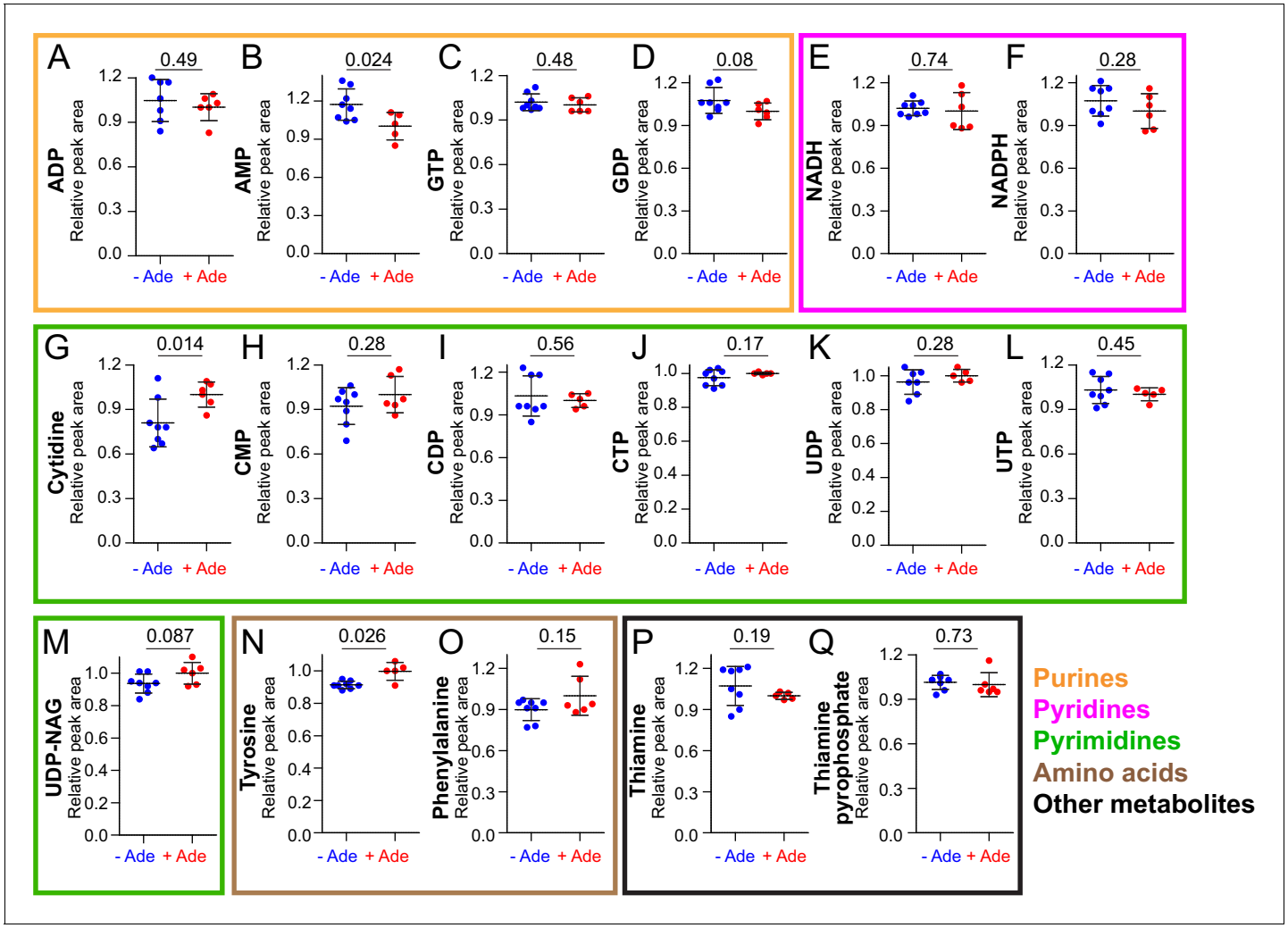

Figure 2—figure supplement 3. Quantification of metabolites not or poorly significantly affected by extracellular purine availability. Results were obtained on the prototrophic wild-type strain FY4 as in ***Figure 2***. Quantifications were determined on independent metabolite extractions (N ≥ 5) and standard deviation is presented. For each metabolite, the amount measured in cells grown in the presence of adenine (red dots) was set at one and p-values indicated on the top of each panel were calculated from a Welch's t-test.

DOI: https://doi.org/10.7554/eLife.43808.008

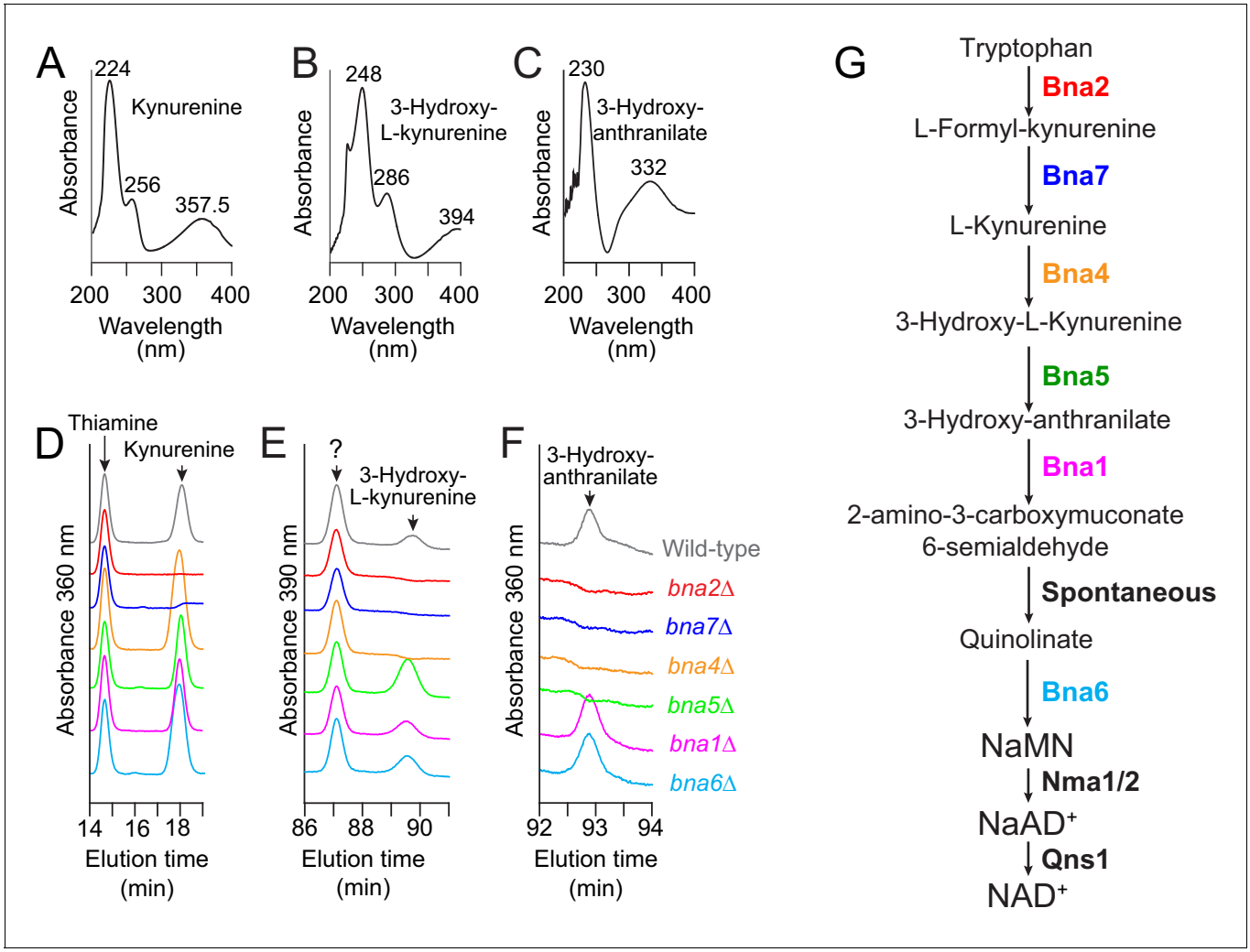

Figure 2—figure supplement 4. Identification of NAD^+ de novo pathway intermediates. (**A–C**) Absorption spectra observed for some NAD^+-de novo pathway intermediates in the ion chromatography conditions used. Values indicate the wavelength of absorption maxima (in nm). (**D–F**) Identification of the peaks corresponding to kynurenine, 3-hydroxy-L-kynurenine and 3-hydroxy-anthranilate using *bna* knock-out mutants. Wild-type (BY4742) and *bna*-mutant (*bna2*: Y10838; *bna7*: Y10904; *bna4*: Y5822; *bna5*: Y10903; *bna1*: Y10901 and *bna6*: Y5891) strains were exponentially grown in SDcasaWAU medium for 24 hr, harvested by filtration and shifted for 7 hr in SDcasaWAU medium lacking nicotinic acid (see Materials and methods section). Metabolite extraction and separation by liquid chromatography were performed as in ***Figure 2***. Panels correspond to the chromatogram sections containing peaks of interest. (**G**) Simplified representation of the NAD^+ de novo pathway showing the block occasioned by each *bna* mutant. NaMN: nicotinic acid mononucleotide. $NaAD^+$: nicotinic acid adenine dinucleotide. Of note, L-Formyl-kynurenine and quinolinic acid could not be detected in our experimental setup.

DOI: https://doi.org/10.7554/eLife.43808.010

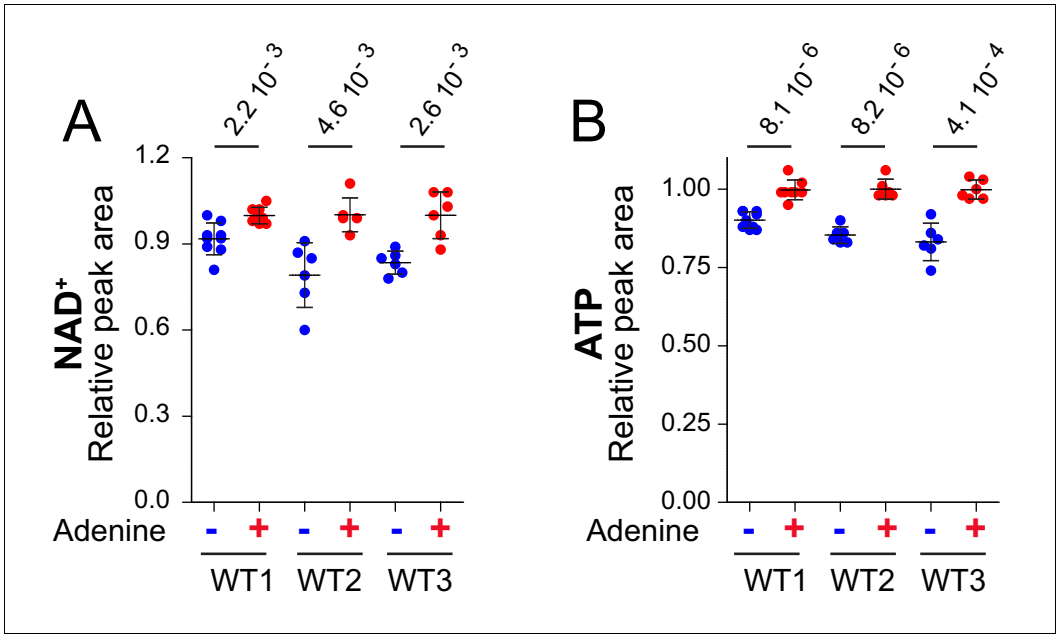

Figure 2—figure supplement 5. NAD^+ and ATP variation in response to adenine availability in wild-type strains. Wild-type (WT1: FY4; WT2: Y286; WT3: BY4742) strains were maintained in exponential growth phase for 24 hr in SDcasaWU supplemented (red dots) or not (blue dots) with adenine. Metabolite extraction, separation and quantification were done as in ***Figure 2***. Quantifications were determined on independent metabolite extractions ($N \geq 5$) and standard deviation is presented. The amount of each metabolite measured in cells grown in the presence of adenine (red dots) was set at one and p-values indicated on the top of each panel were determined by a Welch's t-test.

DOI: https://doi.org/10.7554/eLife.43808.011

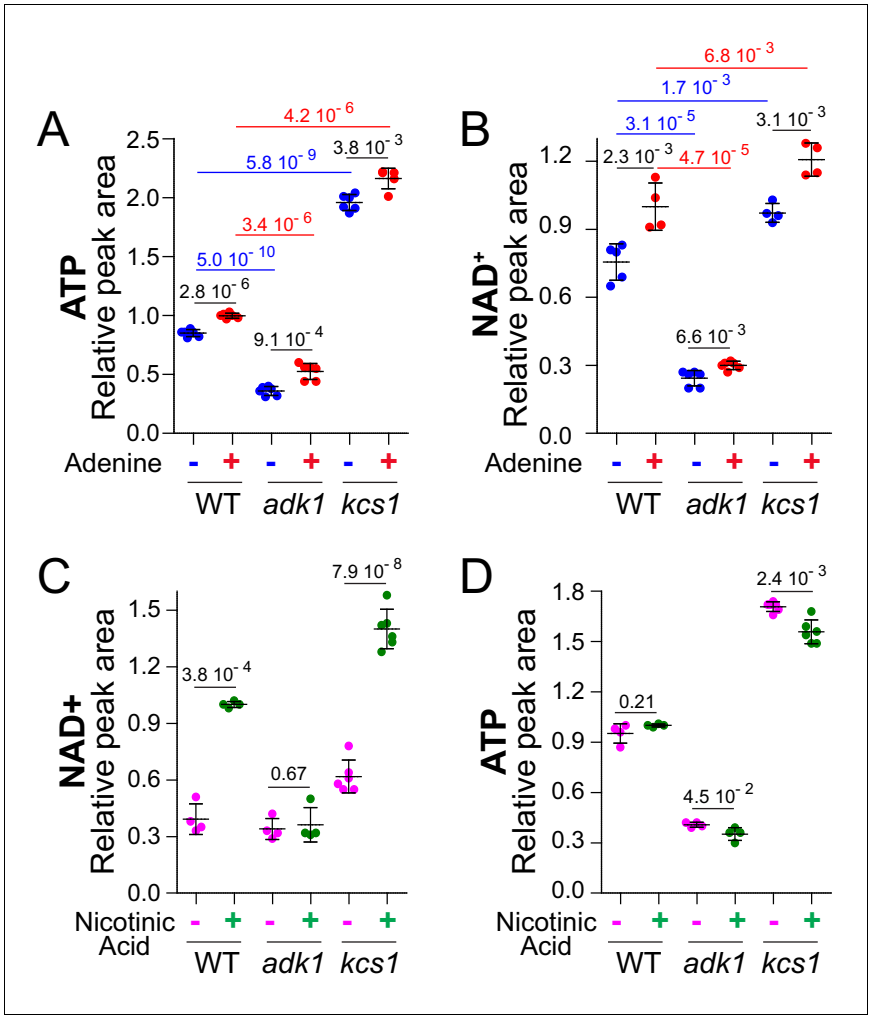

Figure 3. ATP controls NAD$^+$level in yeast. (**A–B**) Intracellular NAD$^+$ varies concomitantly with ATP. Wild-type (BY4742), *adk1* (Y10991) and *kcs1* (Y2337) strains were grown in exponential phase for 24 hr in SDcasaWU medium supplemented (red dots) or not (blue dots) with adenine. The amount of metabolites measured in wild-type cells grown in the presence of adenine (red dots) was set at 1. (**C–D**) Nicotinic acid (NA) supplementation leads to an increase in NAD$^+$ amount in wild-type cells. Cells (wild-type (WT): BY4742, *adk1*: Y10991 and *kcs1*: Y2337) were exponentially grown for 24 hr in SDcasaWU-NA supplemented (green dots) or not (pink dots) with nicotinic acid (400 µg/l). Metabolite amounts measured in wild-type cells grown in the presence of nicotinic acid were set at 1. A-D, Metabolite extraction, separation and quantification were performed as in ***Figure 2***. Quantifications were determined on independent metabolite extractions (N $\geq$ 4) and standard deviation is presented. Numbers on the top of each panel correspond to the p-values determined by a Welch's t-test.

DOI: https://doi.org/10.7554/eLife.43808.014

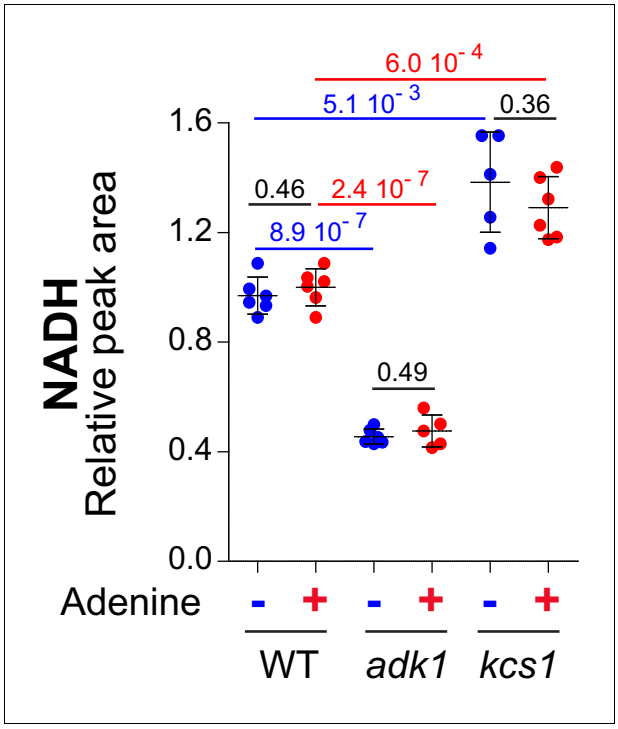

Figure 3—figure supplement 1. NADH varies concomitantly with ATP in *adk1* and *kcs1* knock-out mutants. Results were obtained from the metabolic extraction and separation described in ***Figure 3A–B*** (N $\geq$ 4). The amount measured in cells grown in the presence of adenine (red dots) was set at 1. Error bars correspond to standard deviation and indicated p-values were calculated from a Welch's t-test.

DOI: https://doi.org/10.7554/eLife.43808.015

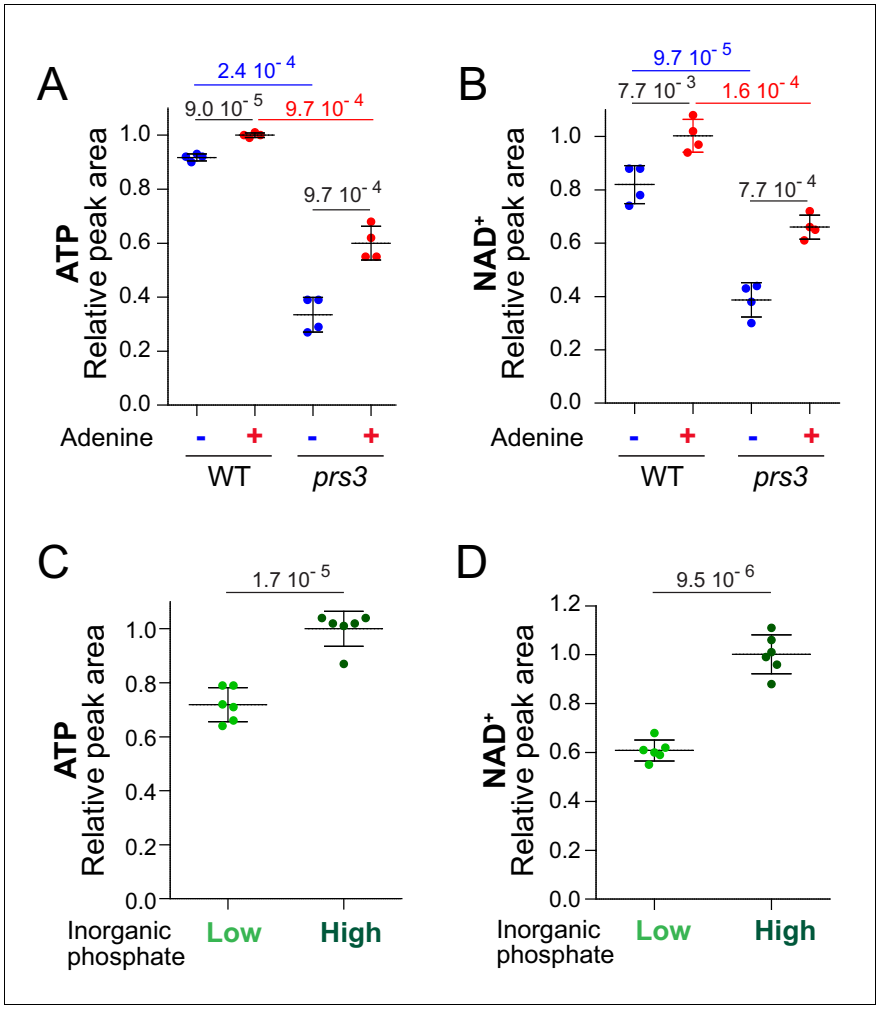

Figure 3—figure supplement 2. Robust correlation between ATP and NAD$^+$variations in diverse ATP-limiting conditions. ATP and NAD$^+$ variations were measured in a wild-type strain (BY4742; **A–D**) and a *prs3* (Y4835; **A–B**) mutant. (**A–B**) Strains were grown in exponential phase for 24 hr in SDcasaWU medium supplemented (red dots) or not (blue dots) with adenine. The amount measured in cells grown in the presence of adenine (red dots) was set at 1. (**C–D**) A prototrophic strain (FY4) was exponentially grown for 24 hr in SD medium containing two concentrations of inorganic phosphate (100 µM: Low, light-green dots; 7.3 mM: High, dark-green dots). The amount measured in cells grown in 7.3 mM phosphate (dark green dots, concentration commonly supplied in yeast defined media) was set at 1. (**A–D**) Independent metabolic extraction (N $\geq$ 4) and separation were performed as in ***Figure 2***. Error bars correspond to standard deviation and indicated p-values were calculated using a Welch's t-test.

DOI: https://doi.org/10.7554/eLife.43808.017

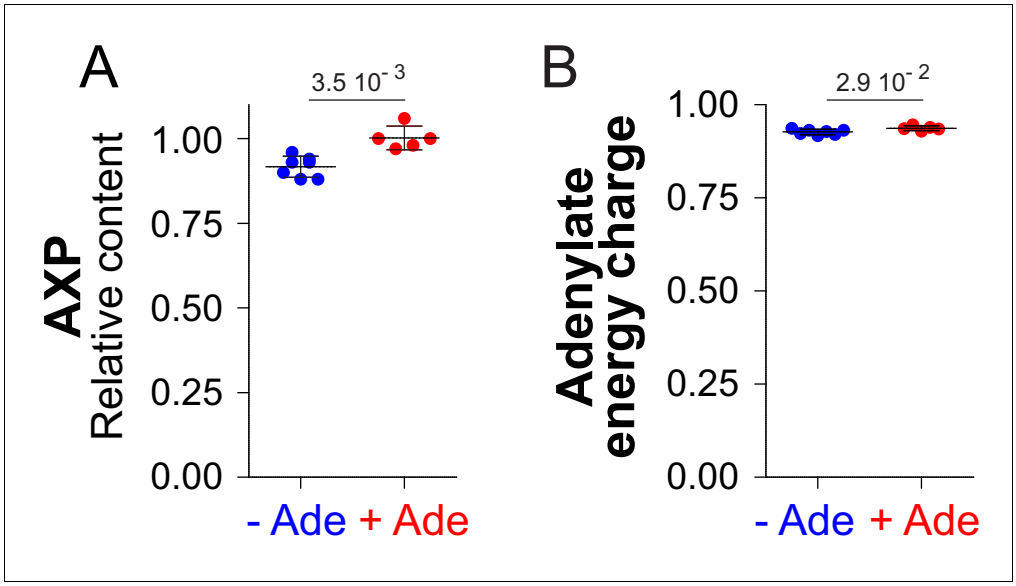

Figure 3—figure supplement 3. Variation of AXP and adenylate energy charge in response to adenine availability. AXP and adenylate energy charge were calculated, as described in the Material and methods section, from metabolic analyses presented in ***Figure 2*** and ***Figure 2—figure supplement 3***. For both parameters, values obtained in the presence of adenine (red dots) were set at one and indicated p-values were calculated using a Welch's t-test ($N \geq 5$).

DOI: https://doi.org/10.7554/eLife.43808.020

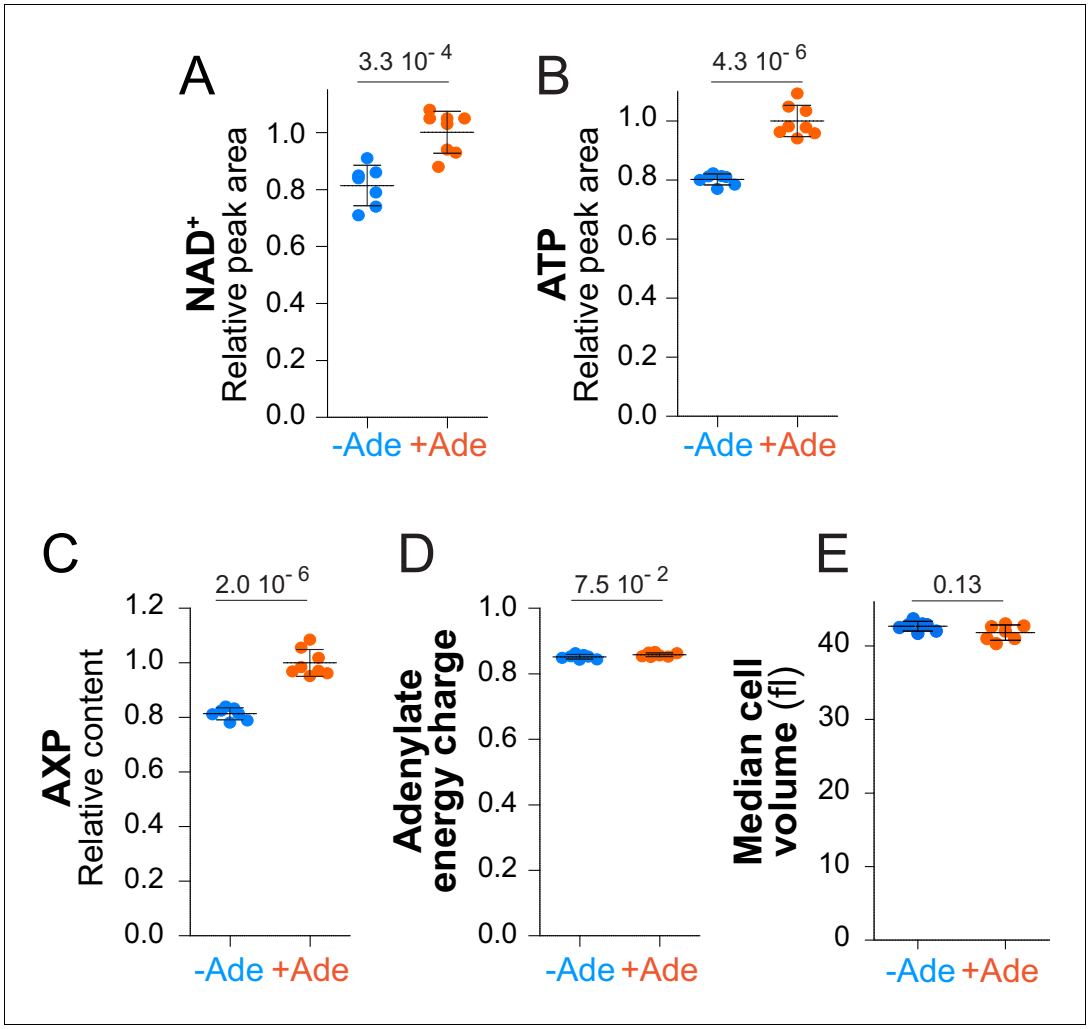

Figure 3—figure supplement 4. NAD^+, ATP, AXP, adenylate energy charge and median cell volume variations in response to adenine availability under respiratory conditions. (**A–D**) The prototrophic wild-type strain (FY4) was exponentially grown for 24 hr in SGEcasaWU supplemented (orange dots) or not (blue dots) with adenine. Metabolite extraction, separation and quantification were done as in ***Figure 2***. Quantifications were determined from independent metabolite extractions ($N \geq 7$) and standard deviation is presented. The amount of each metabolite measured in cells grown in the presence of adenine (orange dots) was set at 1. Indicated p-values were calculated using a Welch's t-test. AXP and adenylate energy charge were determined as described in the Materials and methods section. (**E**) Median cell volume was determined with a Multisizer IV (Beckman coulter) on the independent cell cultures used for the metabolic extraction presented in this figure ($N \geq 7$).

DOI: https://doi.org/10.7554/eLife.43808.022

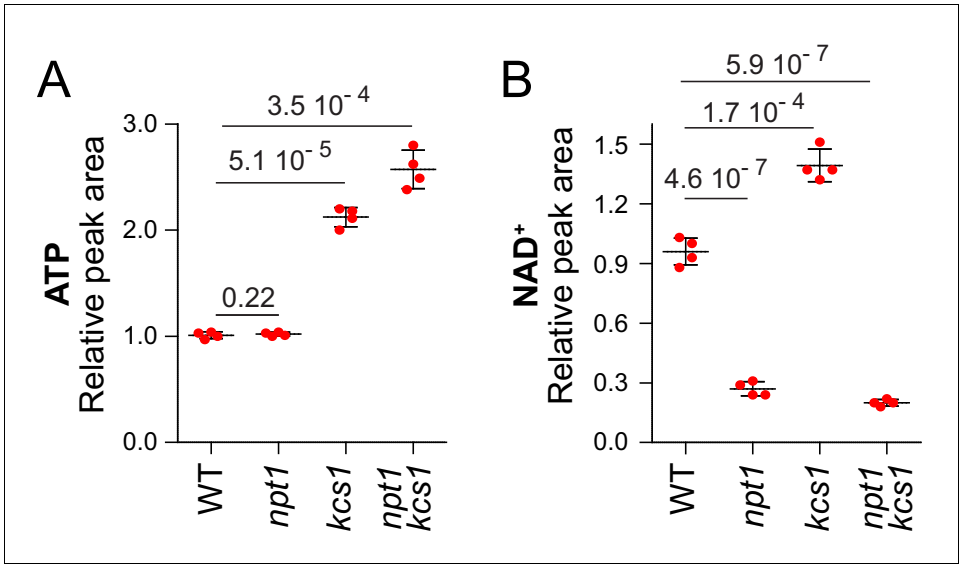

Figure 3—figure supplement 5. Stimulation of NAD$^+$synthesis by ATP is abolished in *npt1* mutants. (**A–B**) Wild-type (WT, Y286), *npt1* (Y5581), *kcs1* (Y2337), and *kcs1 npt1* (Y11017) cells exponentially grown for 24 hr in SDcasaWAU medium. Quantifications (set at one for the amount measured in WT cells) were performed on independent metabolic extractions (N = 4). Error bars correspond to standard deviation and indicated p-values were calculated using a Welch's t-test.

DOI: https://doi.org/10.7554/eLife.43808.025

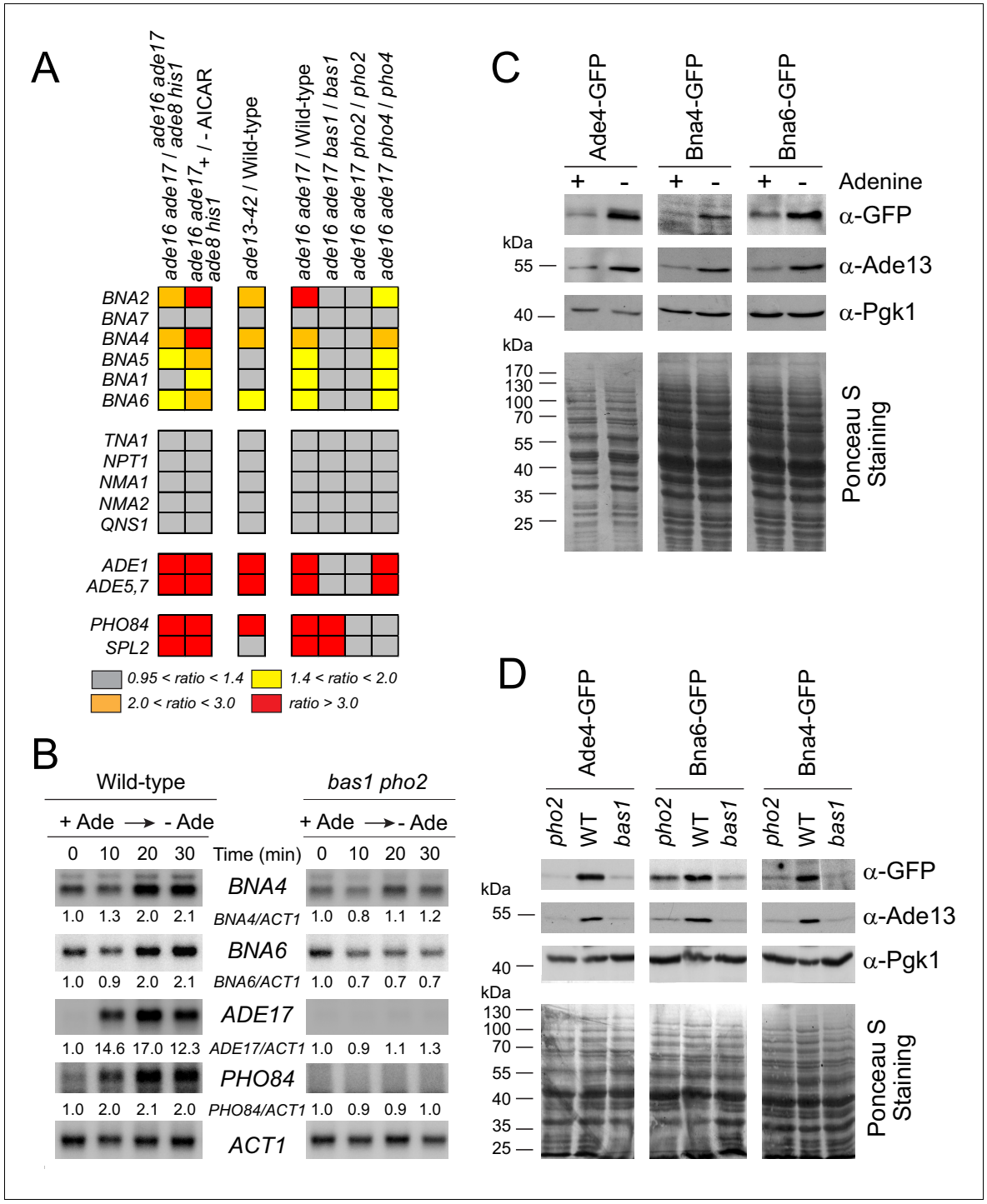

Figure 4. Bas1 and Pho2 transcriptionally upregulate the *BNA* genes in response to (S)ZMP. (**A**) Heat-map representation of the expression of the pyridine pathway genes. Results were extracted from our previously reported microarray analyses (***Hürlimann et al., 2011***; ***Pinson et al., 2009***). Raw data are available at http://www.ncbi.nlm.nih.gov/geo/query/acc.cgi?acc= GSE13275 and https://www.ncbi.nlm.nih.gov/geo/queryacc.cgi?acc= GSE29324. (**B**) Kinetic analysis of *ADE17*, *PHO84* and *BNA* genes expression in a wild-type and a *bas1 pho2* double mutant upon adenine depletion. Wild-type (BY4742) and *bas1 pho2* mutant (Y1487) cells were grown in SDcasaWU + adenine medium, centrifuged for 2 min at 3500 g, washed twice with SDcasaWU and re-suspended in the same medium lacking adenine (time 0). Aliquots were taken at indicated times, total RNA were extracted and gene expression was monitored by Northern blotting (N ≥ 2). Images shown correspond to one representative experiment. (**C–D**) Bna4 and Bna6 proteins are more abundant in adenine-depleted conditions in wild-type cells (**C**) but not in the absence of the Bas1 and Pho2 transcription factors (**D**). (**C**) Wild-type cells harboring either *ADE4* (Y11325), *BNA4* (Y11328), or *BNA6* (Y11327) -GFP fusion at the corresponding gene locus were exponentially

Figure 4 continued on next page

Figure 4 continued

grown for 24 hr in SDcasaWU medium supplemented (+) or not (-) with adenine. (**D**) Wild-type, *bas1* and *pho2* yeast strains harboring either *ADE4* (Y11325, Y11885 and Y11879), *BNA4* (Y11328, Y11894 and Y118887) or *BNA6* (Y11327, Y11885 and Y11890) -GFP fusion at the corresponding gene locus were exponentially grown for 24 hr in SDcasaWAU medium, filtered and then shifted for 2 hr in SDcasaWU medium. (**C–D**) Total proteins were extracted, separated by SDS-PAGE, electro-transferred and revealed by western-blotting using anti-GFP (1/500 (**C**); 1/2,500 (**D**)), anti-Ade13 (1/1200,000) and anti-Pgk1 (1/50,000) antibodies. Ade4-, Bna4- and Bna6-GFP fusions proteins were revealed at 84, 79 and 60 kDa, respectively. Images shown correspond to one representative experiment ($N \geq 2$).

DOI: https://doi.org/10.7554/eLife.43808.029

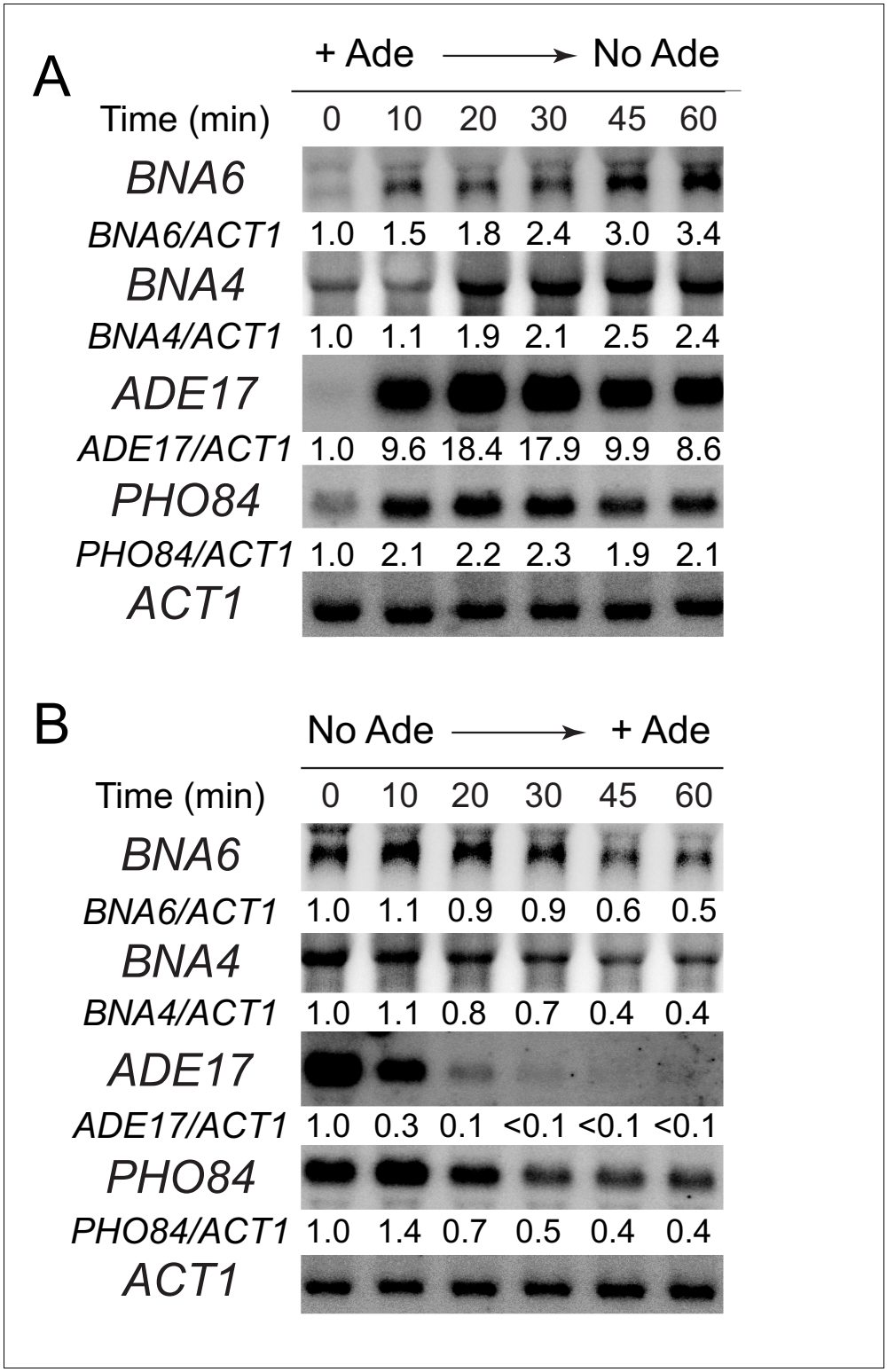

Figure 4—figure supplement 1. Kinetic analysis of *ADE17*, *PHO84* and *BNA* genes expression upon either external adenine depletion (**A**) or addition (**B**). (**A**) Wild-type cells (BY4742) were grown in SDcasaWU + adenine medium, centrifuged for 2 min at 3500 g, washed twice with SDcasaWU and re-suspended in the same medium lacking adenine (time 0). Aliquots were taken at indicated times and gene expression was monitored as in A (N = 1). (**B**) Wild-type cells (BY4742) were exponentially grown in SDcasaWU medium and adenine was added

Figure 4—figure supplement 1 continued on next page

Figure 4—figure supplement 1 continued

(time 0). Total RNA were extracted and gene expression was monitored by northern blotting on aliquots collected at indicated time (N = 1).

DOI: https://doi.org/10.7554/eLife.43808.030

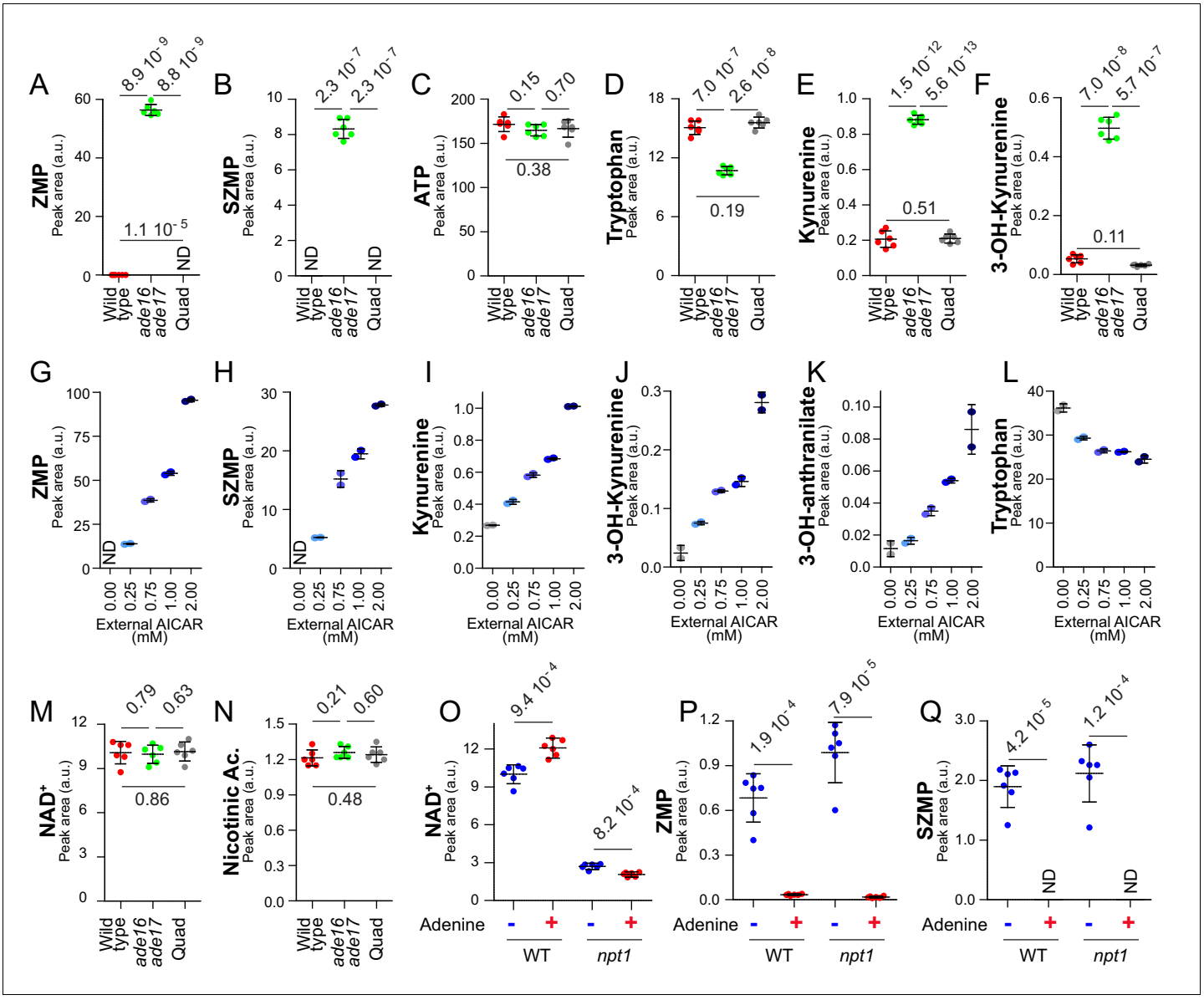

Figure 5. (S)ZMP-increase is sufficient to stimulate the NAD$^+$ *de novo* pathway. (**A–F**) (S)ZMP accumulation in the *ade16 ade17* mutant is associated to a significant increase in NAD$^+$ *de novo* pathway intermediates. Wild-type (BY4742, red dots), *ade16 ade17* (Y1162, green dots) and *ade16 ade17 ade8 his1* (quad; Y2950, grey dots) were grown in SDcasaWAU medium. (**G– L**) Accumulation of ZMP achieved by external AICAR addition correlates with increasing amounts of NAD$^+$ *de novo* pathway intermediates. The *ade16 ade17 ade8 his1* quadruple mutant strain (Y2950) was grown in SDcasaWAU medium and incubated for 24 hr with indicated amounts of AICAR prior to metabolite extraction. (**M–N**) (S)ZMP accumulation has no significant effect on NAD$^+$ and nicotinic acid levels when the salvage pathway is active. NAD$^+$ and nicotinic acid levels were determined from the experiment described in ***Figure 5A–F***. (**O–Q**) Upregulation of the purine de novo pathway in the absence of adenine, when (S)ZMP is high, results in higher intracellular NAD$^+$ only when the pyridine salvage pathway is inactivated. Wild-type (BY4742) and *npt1* knock-out (Y5581) strains were exponentially grown for 24 hr in SDcasaWU medium ±Adenine. (**A–F, M–Q**) Quantifications were determined from independent metabolite extractions (N = 5). Error bars correspond to standard deviation and indicated p-values were calculated from a Welch's t-test.

DOI: https://doi.org/10.7554/eLife.43808.033

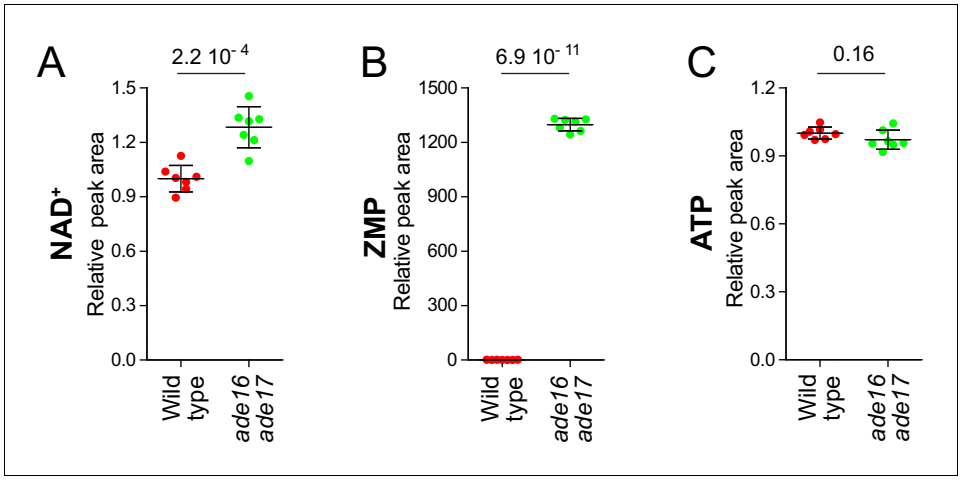

Figure 5—figure supplement 1. NAD^+ level is significantly increased in the *ade16 ade17* (S)ZMP accumulating mutant in the absence of external nicotinic acid. Wild-type (BY4742, red dots) and *ade16 ade17* (Y1162, green dots) were exponentially grown for 24 hr in SDcasaWAU medium lacking nicotinic acid. Metabolite extraction, separation and quantification were done as in ***Figure 2***. Quantifications were determined from independent metabolite extractions ($N \geq 7$) and standard deviation is presented. Values measured in wild-type cells (red dots) were set at 1. Indicated p-values were calculated using a Welch's t-test.

DOI: https://doi.org/10.7554/eLife.43808.034

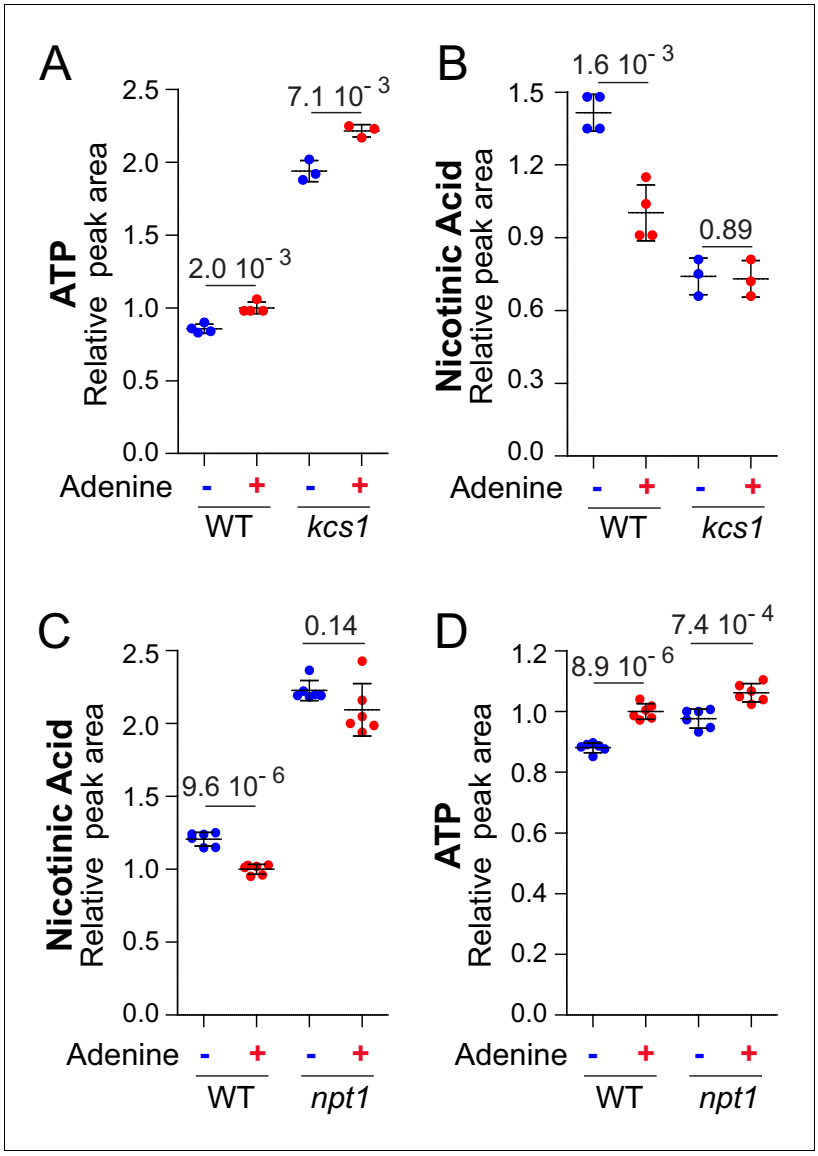

Figure 6. Metabolization of nicotinic acid is tightly connected to the amount of ATP. Nicotinic acid utilization is increased when ATP is higher (**A–B**) and not anymore affected by extracellular adenine in a *npt1* mutant (**C–D**). (**A–D**) Wild-type (BY4742; (**A–D**) and either *kcs1* (Y2337; **A–B**) or *npt1* (Y5581; **C–D**) knock-out mutant strains were exponentially grown for 24 hr in SDcasaWU medium supplemented (red dots) or not (blue dots) with adenine. Quantifications were determined from independent metabolite extractions (N $\geq$ 3) and standard deviation is presented. For each metabolite, the amount measured in wild-type cells grown in the presence of adenine was set at one and indicated p-values were calculated from a Welch's t-test.

DOI: https://doi.org/10.7554/eLife.43808.039

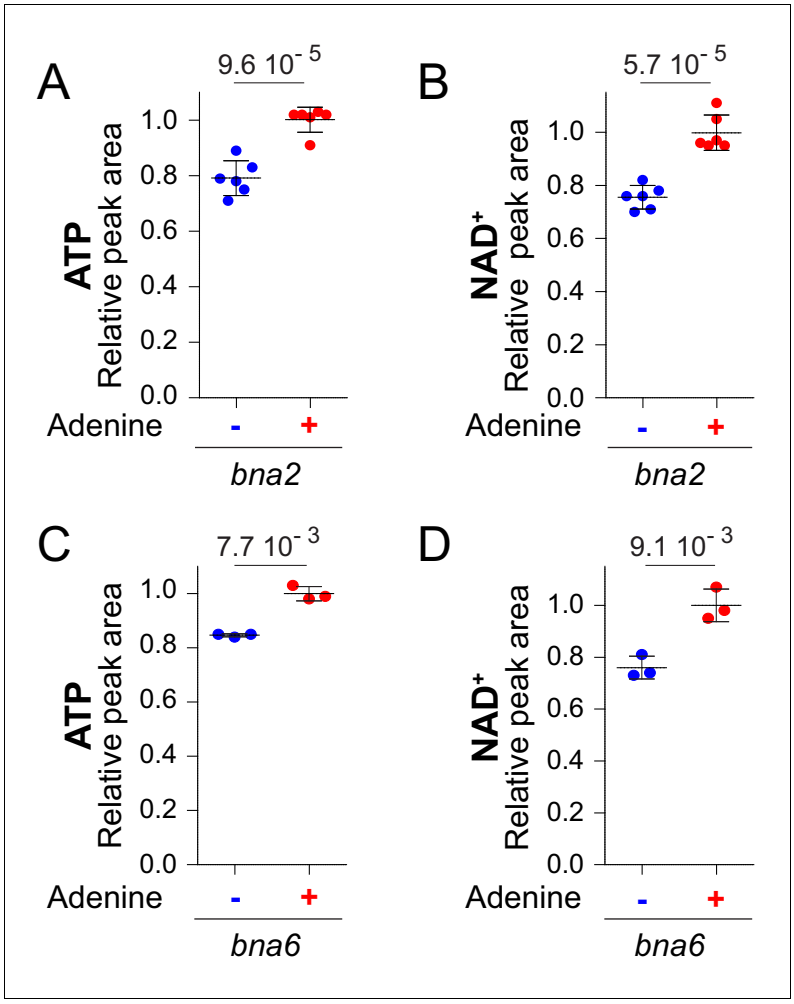

Figure 6—figure supplement 1. NAD^+variations in response to external adenine availability do not require a functional pyridine de novo pathway. ATP (**A–C**) and NAD^+ (**B–D**) levels were determined from *bna2* (Y10838) and *bna6* (Y5891) knock-out mutants exponentially grown for 24 hr in SDcasaWU supplemented (red dots) or not (blue dots) with adenine. Quantifications were determined from independent metabolite extractions (A-B: N = 6; C-D: N = 3) and standard deviation is presented. Metabolite amount measured in cells grown in the presence of adenine (red dots) was set at 1. A Welch's t-test was used to determine the indicated p-values.

DOI: https://doi.org/10.7554/eLife.43808.040

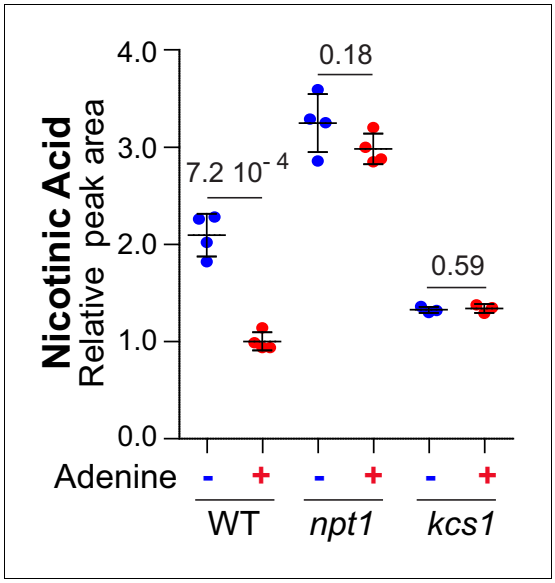

Figure 6—figure supplement 2. Nicotinic acid variations in response to external adenine availability are abolished in *npt1* and *kcs1* mutants fed with nicotinamide. Wild-type (BY4742) and knock-out mutant strains (*npt1*: Y5581 and *kcs1*: Y2337) were exponentially grown for 24 hr in SDcasaWU-NA medium (lacking nicotinic acid), supplemented with nicotinamide, as an external pyridine source, and containing (red dots) or not (blue dots) adenine. Quantifications were determined from independent metabolite extractions (N $\geq$ 3) and standard deviation is presented. The amount measured in wild-type cells grown in the presence of adenine was set at one and indicated p-values were calculated from a Welch's t-test.

DOI: https://doi.org/10.7554/eLife.43808.042

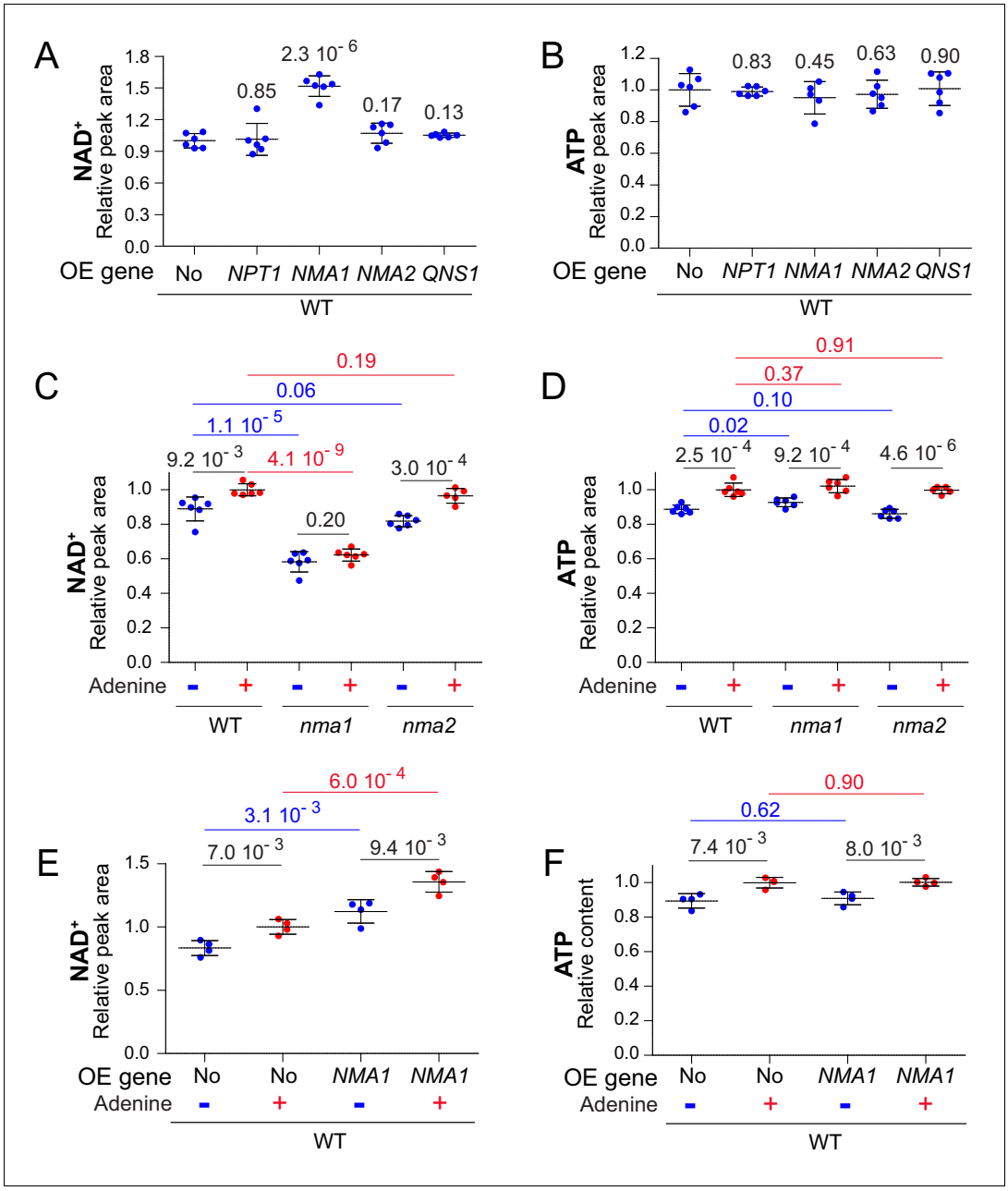

Figure 7. Nicotinic acid mononucleotide adenylyl transferase activity limits NAD^+ synthesis. (**A–B**) Overexpression of *NMA1* is sufficient to increase NAD^+ content when cells are grown in the absence of adenine. Wild-type cells (BY4742) were transformed with plasmid allowing overexpression (OE) of the indicated pyridine salvage pathway genes or the empty vector (No). Transformants were grown in SDcasaWU medium lacking adenine. Values obtained with the empty vector were set at 1. (**C–D**) NAD^+ does not respond to adenine availability in cells lacking *NMA1*. Wild-type cells (BY4742) and *nma* mutants (*nma1*: Y5662; *nma2*: Y5663) strains were grown in SDcasaWU medium lacking (blue dots) or not (red dots) adenine. Values obtained in the wild-type strain grown in the presence of adenine were set at 1. (**E–F**) Overexpression of *NMA1* leads to increased intracellular NAD^+. Wild-type cells (BY4742) were transformed with a plasmid allowing overexpression (OE) of *NMA1* gene or the empty vector (No). Transformants were grown in SDcasaWU medium lacking (blue dots) or not (red dots) adenine. Values obtained with the empty vector in the presence of adenine were set at 1. (**A–F**) Quantifications were determined independent metabolite extractions ($N \geq 4$) and standard deviation is presented. Indicated p-values were calculated from a Welch's t-test.

DOI: https://doi.org/10.7554/eLife.43808.046

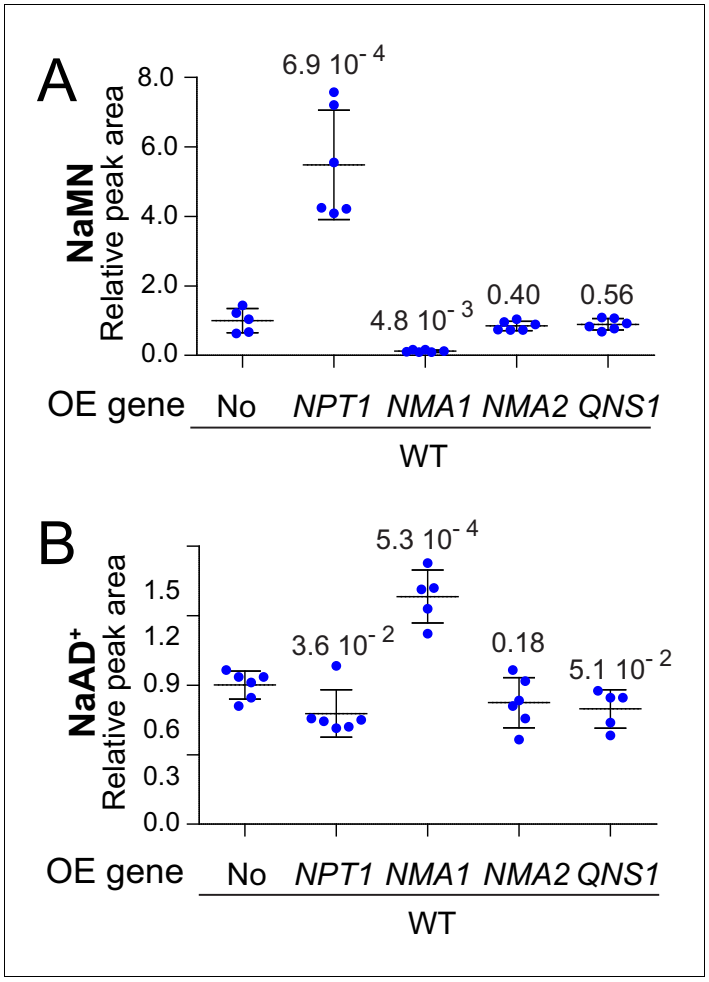

Figure 7—figure supplement 1. NaMN and NaAD$^+$are increased in response to *NPT1* and *NMA1* genes overexpression, respectively. Wild-type cells (BY4742) were transformed with plasmids allowing overexpression (OE) of the indicated pyridine salvage pathway genes or the empty vector (No). Transformants were grown in SDcasaWU medium lacking adenine. Values obtained with the empty vector were set at 1. Quantifications were determined from independent metabolite extractions (N $\geq$ 5), standard deviation is presented and p-values were calculated from a Welch's t-test.

DOI: https://doi.org/10.7554/eLife.43808.047

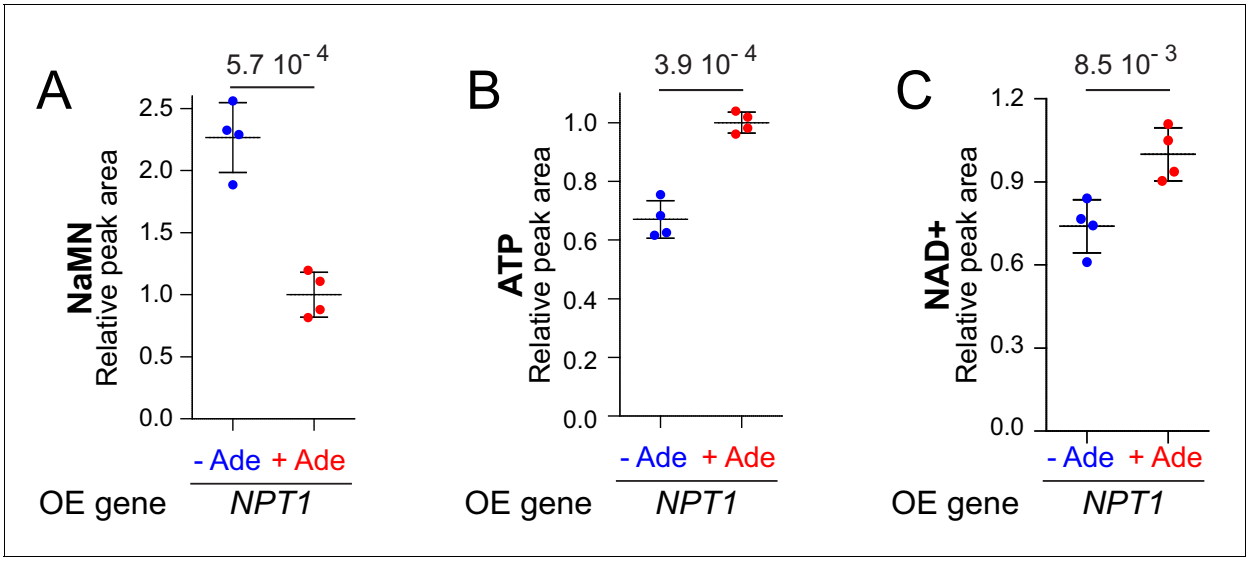

Figure 7—figure supplement 2. Accumulation of NaMN in response to *NPT1* overexpression is higher when ATP is limiting. Wild-type cells (BY4742) were transformed with a plasmid allowing overexpression (OE) of the *NPT1* gene. Transformants were grown in SDcasaWU medium lacking (blue dots) or not (red dots) adenine. Values obtained with the empty vector were set at 1. Quantifications were determined from independent metabolite extractions (N = 4). Standard deviation is presented and indicated p-values were calculated using a Welch's t-test.

DOI: https://doi.org/10.7554/eLife.43808.049

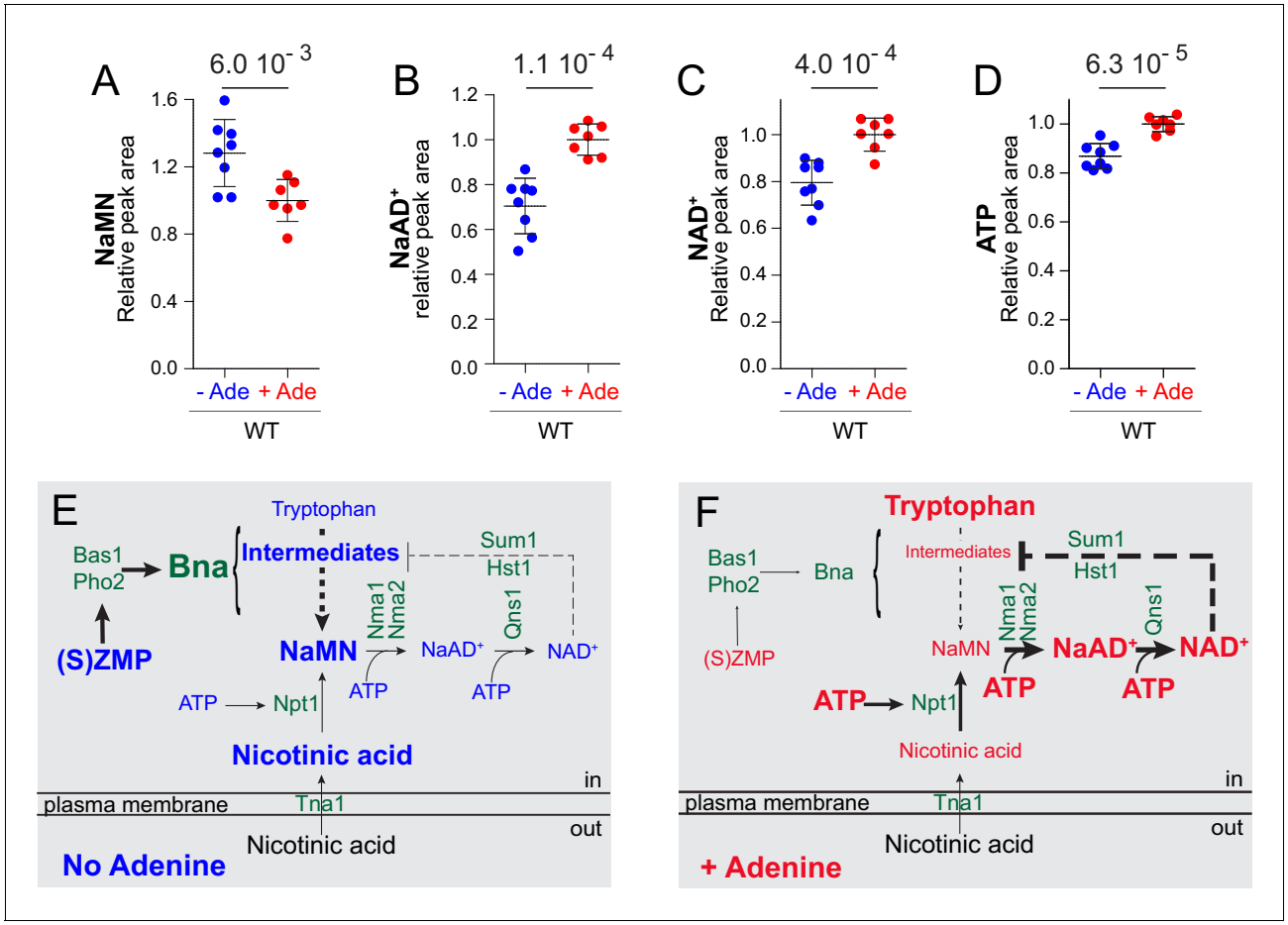

Figure 8. Yeast co-regulates purine and pyridine metabolism in response to adenine through two mechanisms. (**A–D**) The Nma1-bottleneck for NAD^+ synthesis operates under physiological conditions. A prototrophic strain (FY4) was grown in SDcasaWU medium lacking (blue dots) or not (red dots) adenine. Values obtained in the presence of adenine (red dots) were set at one for each metabolite. Quantifications were determined from independent metabolite extractions ($N \geq 7$). Standard deviation is presented and a Welch's t-test was used to calculate the indicated p-values. (**E–F**) Model of NAD^+ synthesis rerouting in response to extracellular adenine availability. The thickness of lines and arrows refers to the intensity of signaling or flux in metabolic pathways. For each metabolite, the font-size reflects variation of its intracellular content.

DOI: https://doi.org/10.7554/eLife.43808.054

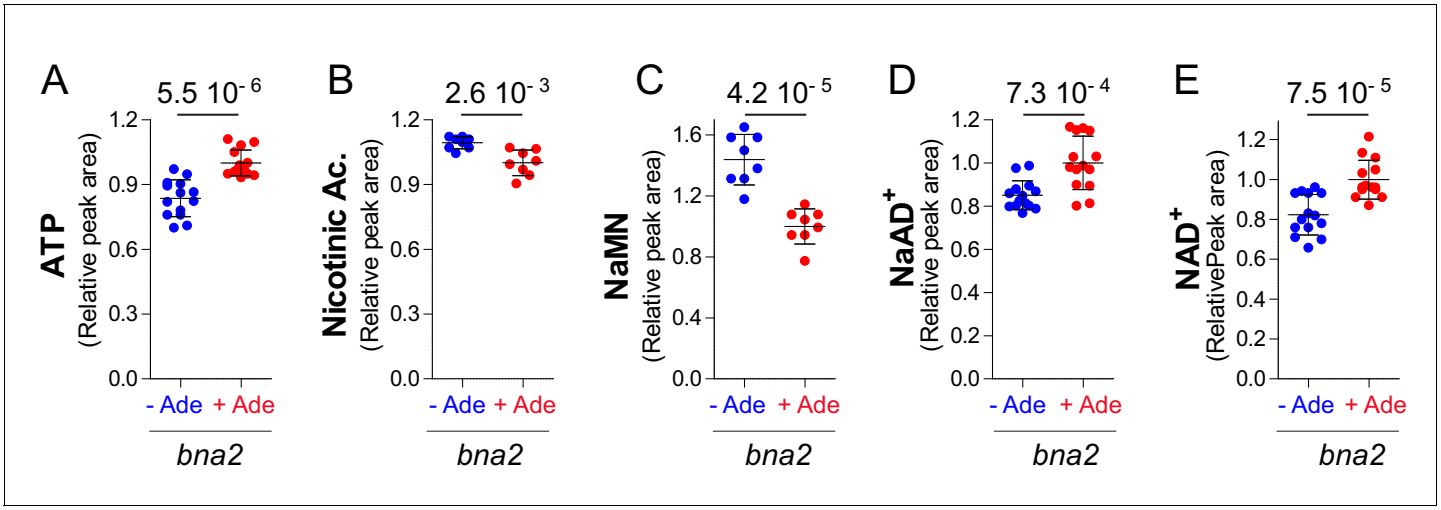

Figure 8—figure supplement 1. Modulation of adenine on NAD$^+$biosynthesis operates in the absence of a functional de novo pathway. Pyridine salvage intermediate levels were determined in a *bna2* mutant strain (Y11838) exponentially grown for 24 hr in SDcasaWU medium lacking (blue dots) or not (red dots) adenine. Values obtained in the presence of adenine (red dots) were set at 1. Quantifications were determined from independent metabolite extractions (N $\geq$ 8). Standard deviation is presented and indicated p-values were calculated using a Welch's t-test.

DOI: https://doi.org/10.7554/eLife.43808.055